Downlink Transmission of Broadband OFCDM Systems—Part III: Turbo-Coded

Yiqing Zhou, *Member, IEEE*, Jiangzhou Wang, *Senior Member, IEEE*, and Mamoru Sawahashi, *Member, IEEE*

***Abstract*—Orthogonal frequency and code-division multiplexing (OFCDM) systems have been introduced for high-speed data transmission in future wireless mobile communications. In this paper, a hybrid multicode interference cancellation (MCI) and minimum mean-square error (MMSE) detection scheme is presented for the turbo-coded OFCDM systems. Channel estimation based on a code-multiplexed pilot channel is employed. The weights of the hybrid detection are derived theoretically and an effective method to generate the weights in practical applications is proposed. By means of computer simulation, the effects of system parameters on the performance are studied extensively. It is shown that the hybrid detection outperforms pure MMSE detection in various channel conditions, especially for high-level modulation schemes. To carry out interference regeneration for the hybrid detection, the conventional turbo decoding algorithm which only decodes systematic bits should be extended to decode parity bits as well. Moreover, two iterations in turbo decoding are sufficient to provide good performance for the system with the multistage hybrid detection. Finally, given time-domain spreading factor N_T, the system performance improves with frequency-domain spreading factor N_F. However, the frequency diversity gain is saturated when N_F is large (i.e., $N_F \geq 16$).**

***Index Terms*—Interference cancellation, minimum mean-square error (MMSE) detection, orthogonal frequency-division multiplexing (OFDM), turbo codes.**

I. Introduction

THE ERA OF high-speed data transmission in mobile communications is approaching rapidly. Coupled with enhanced techniques, the fourth-generation (4G) wireless network aims to provide ultra-high-speed data transmissions, such as 100 Mb/s, especially, in downlink. The orthogonal frequency and code-division multiplexing (OFCDM) system [1] is one of the promising candidates for downlink broadband 4G wireless access. Based on orthogonal frequency-division multiplexing (OFDM) techniques, the OFCDM system is robust to the severe multipath interference in a broadband wireless channel. Moreover, the OFCDM system employs two-dimensional (2-D) spreading: time-domain spreading and frequency-domain spreading. Each data symbol in the OFCDM system is spread in time-domain with N_T chips and in frequency-domain with N_F chips. Therefore, totally $N = N_T \times N_F$ spread chips per data symbol are involved in the 2-D spreading.

Manuscript received October 14, 2004; revised May 26, 2005. This paper was presented in part at WirelessCom 2005, Maui, HI, June 2005.

Y. Zhou and J. Wang are with Department of Electrical and Electronic Engineering, University of Hong Kong, Hong Kong (e-mail: yqzhou@eee.hku.hk; jwang@eee.hku.hk).

M. Sawahashi is with IP Radio Network Development Department, NTT DoCoMo, Inc., Kanagawa 239-8536, Japan (e-mail: sawahasi@mlab.yrp.nttdocomo.co.jp).

Digital Object Identifier 10.1109/JSAC.2005.858876

The OFCDM system employs multicode techniques as an efficient way to achieve ultra-high-speed data transmission in downlink. That is, when a user requests for high-speed multimedia services, the base station may allocate multiple or even all available code channels to this user to provide the high-speed transmission. The system adopts packet switch instead of circuit switch, so that multiple-user interference does not exist. However, the interference among multiple codes of one single user may occur. Using orthogonal variable spreading factor (OVSF) codes [2], there would be no interference among the multiple code channels in an additive white Gaussian noise (AWGN) channel. However, in a realistic mobile channel, the code orthogonality may be destroyed by the possible fast fading in time-domain and especially the different fading among subcarriers in frequency-domain. Therefore, multicode interference (MCI) will occur. In order to improve the performance, MCI should be cancelled out as much as possible. However, it should be noted that the MCI cancellation in time-domain is difficult because near perfect channel estimation for each time instant is required in the presence of large Doppler shift. Therefore, in time-domain, a simple equal gain combining (EGC) technique is employed and no MCI cancellation will be carried out. On the other hand, in frequency-domain, the MCI is serious. Therefore, MCI cancellation is considered in conjunction with minimum mean-square error (MMSE) detection.

So far, there has been no paper discussing the MCI cancellation in the turbo-coded OFCDM system. Thus, it is desirable to investigate the performance of the coded OFCDM when multistage MCI cancellation is employed. Parallel-type interference cancellation is considered because it is more practical than the serial type due to its short processing delay. Furthermore, interference cancellation can be implemented in either hard decision or soft decision. Although soft decision can provide better performance than hard decision, it is complicated to choose a suitable soft decision function in a channel-coded system. Therefore, hard decision is considered in this paper due to its simple realization in practical systems. Moreover, to carry out coherent detection and multistage MCI cancellation, a good channel estimation technique is needed. Pilot aided channel estimation is considered. In the OFCDM system, there are three types of pilot channels: code-multiplexed, time-multiplexed, and frequency-multiplexed. A code-multiplexed pilot channel is preferred since it provides precise estimations, as well as more flexibility [3].

By combining MMSE detection and parallel interference cancellation techniques in frequency-domain, hybrid MCI cancellation and MMSE detection has been proposed for the uncoded OFCDM system [4]. In the turbo-coded OFCDM

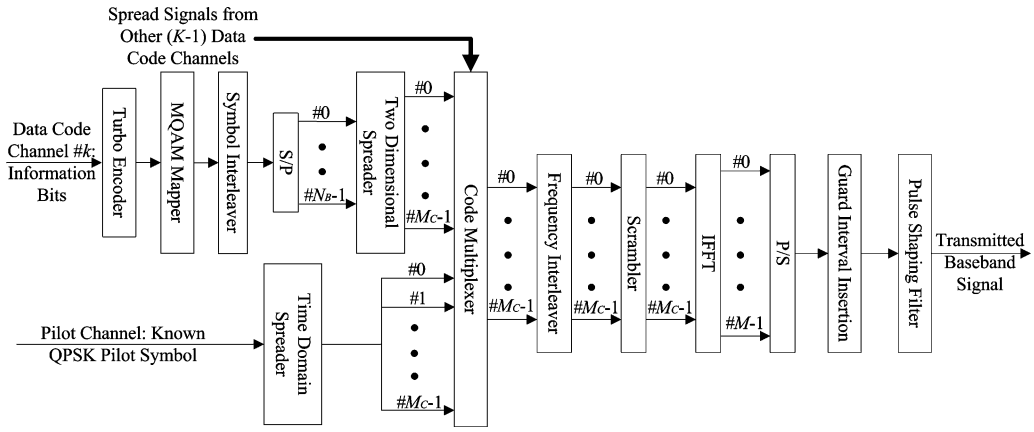

Fig. 1. Transmitter block diagram of OFCDM systems.

system with hybrid detection, the tentative recovered bits after decoding are used to regenerate the MCI replicas. Moreover, the MMSE weight should be updated stage by stage due to the reduction of MCI in the input signals. An effective method to estimate MMSE weights is proposed. The objective of this work is to evaluate the performance of the hybrid detection in the turbo-coded OFCDM systems, when the channel estimation based on a code-multiplexed pilot channel is employed. The effects of key system parameters, such as the number of MCI cancellation stages, the iterations in turbo decoding, the spreading factors, etc., are investigated extensively.

The rest of this paper is organized as follows. Section II describes the OFCDM system and the channel model. The channel estimation technique and the hybrid MCI cancellation and MMSE detection are presented in Section III. Then, computer simulation results are presented in Section IV. Finally, conclusions are drawn in Section V.

II. System Description

A. Transmitter

The packet transmission on the synchronous downlink broadband channel is considered. 2-D OVSF codes are employed as short channelization codes. For the spreading factor $N = N_T \times N_F$, it is assumed that totally K $(K < N)$ 2-D codes are assigned to a user for high-speed data transmission. The 2-D code assigned to the kth channel is denoted as $\{C_{N_T}^{(k_T)}, C_{N_F}^{(k_F)}\}$ as in [4], where $C_{N_T}^{(k_T)} = \{c_{N_T,0}^{(k_T)}, \cdots, c_{N_T,N_T-1}^{(k_T)}\}$ is the time-domain spreading code and $C_{N_F}^{(k_F)} = \{c_{N_F,0}^{(k_F)}, \cdots, c_{N_F,N_F-1}^{(k_F)}\}$ is the frequency-domain spreading code. $C_{N_T}^{(k_T)}$ and $C_{N_F}^{(k_F)}$ are the (k_T)th and (k_F)th codes on the $(\log_2 N_T)$th and $(\log_2 N_F)$th layers, respectively, in the OVSF code tree [2].

At the transmitter side (see Fig. 1), information bits of each data code channel are first turbo encoded [5], then Gray mapped into multilevel quadrature amplitude modulation (MQAM) symbols by a 4 quadrature amplitude modulation (QAM)- [i.e., quadrature phase-shift keying (QPSK)] or 16 QAM-modulator. The resultant symbol sequence is then processed by the symbol interleaver [6]. Interleaved data symbols are serial-to-parallel (S/P) converted into $N_B = M_C/N_F$ streams, where M_C is the total number of subcarriers, N_F of which carry the same data symbol. After S/P conversion, 2-D spreading is carried out, where each data symbol is first spread into N_T chips in time-domain with the spreading code $C_{N_T}^{(k_T)}$, then, the time-domain spread signal is duplicated into N_F copies and multiplied by the frequency-domain spreading code $C_{N_F}^{(k_F)}$. At the same time, the same known QPSK pilot symbol is first spread in time-domain with the pilot code $c_{P,i}$ and spreading factor of $N_{T,P}$, then repeated into M_C streams, corresponding to M_C subcarriers. The spread signals from K data channels and one pilot channel are added together by the code-multiplexer. After that, a frequency interleaver [6] is employed in order for the system to benefit from frequency diversity due to the different fading among interleaved subcarriers. Scrambling is then carried out. The resultant signals will be up-converted into M_C subcarriers by using an M-point IFFT, where $M \geq M_C$ and the value of M is a power of 2. The M_C subcarriers are located in the middle of the inverse fast Fourier transform (IFFT) points and zeros are padded at each side of the M_C points. After IFFT, an effective time chip (or OFCDM symbol) is obtained with M samples, whose duration is $T_e = MT_s$ and T_s is the sampling time. Then, a guard interval of T_g is inserted between OFCDM symbols to prevent intersymbol interference. Therefore, the time duration of a complete OFCDM symbol is $T = T_e + T_g$. Finally, the complete OFCDM symbol passes through the pulse shaping filter, which gives rise to the baseband transmitted signal.

Therefore, the spread modulated data signal on the mth subcarrier in the ith OFCDM symbol duration can be written as

$$S_{k,m,i}(t) = \sqrt{P_d} d_{k,m,i} c_{N_T,i}^{(k_T)} c_{N_F,m}^{(k_F)} s_{m,i} e^{j2\pi f_m (t-iT)} p(t-iT) \quad (1)$$

where P_d is the signal power of one data code on one subcarrier, $d_{k,m,i}$ is the modulated data symbol of the kth data channel with unitary power, $c_{N_T,i}^{(k_T)} c_{N_F,m}^{(k_F)}$ is the 2-D spreading code, $s_{m,i}$ is the cell-specific scrambling code, f_m is the baseband equivalent frequency of the mth subcarrier, and $p(t)$ is the impulse response (unitary rectangular pulse) of the pulse shaping filter. Furthermore, the spread signal on the code-multiplexed pilot channel can be written as

$$S_{P,m,i}(t) = \sqrt{\beta P_d} d_P c_{P,i} s_{m,i} e^{j2\pi f_m (t-iT)} p(t-iT) \quad (2)$$

where β is the power ratio of pilot to one data channel and d_P is the known QPSK modulated pilot symbol with unitary power.

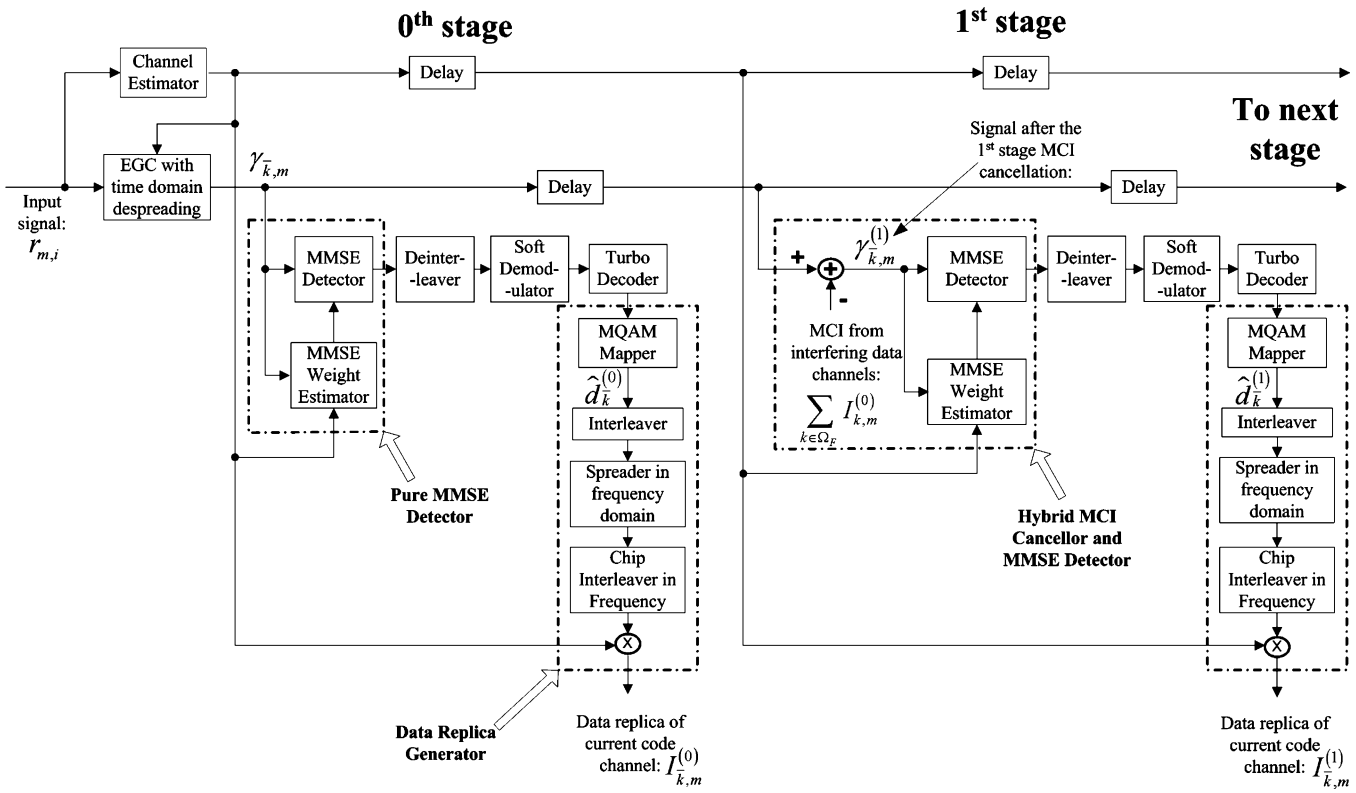

Fig. 2. Receiver block diagram of one data code channel.

Finally, the transmitted signal on the M_C subcarriers in one packet duration is given by

$$S(t)=\sum_{i=0}^{N_d-1}\sum_{m=\frac{(M-M_C)}{2}}^{\frac{(M+M_C)}{2}-1}\left[\sum_{k=0}^{K-1}S_{k,m,i}(t)+S_{P,m,i}(t)\right] \quad (3)$$

where N_d is the number of OFCDM symbols in one packet duration.

In downlink, all code signals are synchronized and experience the same multipath fading channel with the low-pass equivalent impulse response

$$h(t)=\sum_{l=0}^{L-1}h_l(t)\delta(t-\tau_l) \quad (4)$$

where $h_l(t)$ is the complex time-varying channel fading for the lth path and τ_l is the time delay of the lth path, uniformly distributed in $[0,T_g)$. The amplitude and phase of $h_l(t)$ are Rayleigh distributed and uniformly distributed in $[0,2\pi)$, respectively. Furthermore, $h_{l_1}(t)$ and $h_{l_2}(t)$ are assumed to be statistically independent for $l_1 \neq l_2$. Finally, the average frequency response over the ith OFCDM symbol on the mth subcarrier is given by

$$H_m(i)=\sum_{l=0}^{L-1}e^{-j2\pi f_m\tau_l}\left[\frac{1}{T_e}\int_{iT}^{iT+T_e}h_l(t)dt\right], \quad 0\le m\le M-1. \quad (5)$$

B. Receiver

Assuming that the guard interval is larger than the maximum path delay spread, there is no intersymbol interference in the received signals. After passing through a matched filter, down-converted by an FFT block, descrambled and deinterleaved, the received signal on the mth subcarrier in the ith OFCDM symbol duration is denoted as $r_{m,i}$, which is input to K parallel processors, corresponding to K data channels. Fig. 2 shows the receiver block diagram of the $\overline{k}$th data code channel. First of all, the channel fading on each subcarrier is estimated by using the code-multiplexed pilot channel. With the estimated channel information, the EGC weights can be obtained and time-domain despreading is carried out for data channels. At the zeroth stage (without MCI cancellation), using the signals $\gamma_{\overline{k},m}$ after equal-gain combining (EGC) detection, and the estimated channel fading, MMSE weights can be generated. Then, $\gamma_{\overline{k},m}$ is despread in frequency-domain and combined at the MMSE detector using the estimated MMSE weights. After that, the signals are processed by the symbol deinterleaver. To provide soft-valued bit streams to the turbo decoder, a soft MQAM demodulator is needed, where a maximum-a-posterior algorithm (Max_Log_MAP [7]) is employed. Moreover, in a conventional turbo decoder, only the information bits (or *systematic bits*) are concerned. Therefore, only systematic bits are recovered after decoding. However, in the interference cancellation, data replica must be regenerated. Therefore, all coded bits should be recovered. There are two methods to recover the parity bits. One method is to encode the recovered systematic bits. This method is simple but the errors in systematic bits will propagate to parity bits due to the recursive encoder. The other way is to recover

parity bits directly from turbo decoding, using a similar decoding algorithm, as illustrated in [5] and [8]. It will be shown later that without error propagation, the second method provides better performance than the first method. Therefore, the calculation of the logarithm of likelihood ratio (LLR) for parity bits is added in the conventional turbo decoding and this extended algorithm will recover both systematic and parity bits. Based on the outputs of turbo decoder, the tentative data decision on the zeroth stage for the $\overline{k}$th code channel is obtained and denoted as $\hat{d}_{\overline{k}}^{(0)}$. Using $\hat{d}_{\overline{k}}^{(0)}$ and the estimated channel condition, the data replica for the current code channel $I_{\overline{k},m}^{(0)}$ can be generated.

With the replicas of all data channels ($I_{k,m}^{(0)}, k = 0, \cdots, K-1$) at the zeroth stage, hybrid MCI cancellation and MMSE detection can be carried out at the first stage. As shown in Fig. 2, in the hybrid detection, the MCI from interfering data channels, $\sum_{k\in\Omega_F} I_{k,m}^{(0)}$, is cancelled out from the received signal, where Ω_F is the set of 2-D codes which have the same time-domain spreading code as the desired code $\overline{k}$, but different frequency-domain spreading codes from the desired code $\overline{k}$. Then, MMSE weights must be updated due to the MCI reduction in the input signal. Using the new weights of the hybrid detection, the signal after MCI cancellation $\gamma_{\overline{k},m}^{(1)}$ will be processed in the same way as that in the zeroth stage. Similarly, data replicas ($I_{\overline{k},m}^{(1)}$) are generated and used in the next stage for the hybrid detection. Generally speaking, as the decoding outputs become more reliable stage by stage, MCI can be regenerated with higher accuracy stage by stage. After subtraction, MCI can be cancelled out much from the input signal $\gamma_{\overline{k},m}$. Thus, the system performance can be improved stage by stage.

III. Hybrid Detection

A. Channel Estimation and EGC

Channel estimation is carried out on each subcarrier by using the code-multiplexed pilot channel. First of all, the input signal $r_{m,i}$ to the channel estimator on the mth subcarrier in the ith OFCDM symbol duration is given by

$$r_{m,i} = \left(\sum_{k=0}^{K-1} \sqrt{P_d} d_{k,m,i} c_{N_T,i}^{(k_T)} c_{N_F,m}^{(k_F)} + \sqrt{\beta P_d} d_P c_{P,i} \right) s_{m,i} \cdot H_m(i) + \eta_m(i) \quad (6)$$

where $\eta_m(i)$ is sum of the background noise and the intercarrier interference due to Doppler shift. $r_{m,i}$ is then descrambled and despread in time-domain using the pilot code. The preliminary channel fading factor for the mth subcarrier and nth pilot symbol is given by

$$\xi_{m,n} = \frac{1}{N_{T,P}\sqrt{\beta P_d} d_P} \sum_{i=(n-1)N_{T,P}}^{i=nN_{T,P}-1} r_{m,i} c_{P,i} s_{m,i}. \quad (7)$$

In practice, the number of pilot symbols can be small in a packet. When there are three pilot symbols in one packet, three preliminary channel estimations can be obtained from (7). Using $\xi_{m,n}$ ($n = 0, 1, 2$), the channel fading factor on the mth subcarrier in the ith OFCDM symbol duration, $\xi_m(i)$ ($i = 0, 1, \ldots, N_d - 1$), can be approximated by linear interpolation, which is given by

$$\xi_m(i) = \begin{cases} \frac{\xi_{m,1}-\xi_{m,0}}{N_{T,P}} \left(i - \frac{N_{T,P}}{2} \right) + \xi_{m,0}, & 0 \le i < \frac{N_d}{2} \\ \frac{\xi_{m,2}-\xi_{m,1}}{N_{T,P}} \left(i - \frac{3N_{T,P}}{2} \right) + \xi_{m,1}, & \frac{N_d}{2} \le i \le N_d - 1 \end{cases}. \quad (8)$$

Since the channels on adjacent subcarriers in frequency-domain are highly correlated, $\xi_m(i)$ can be averaged over adjacent subcarriers to improve the reliability of channel estimation. Using a sliding window average, the final channel estimation $\hat{H}_m(i)$ for the mth subcarrier in the ith OFCDM symbol duration is given by

$$\hat{H}_m(i) = \frac{1}{2N_{\text{avg}}+1} \sum_{j=m-N_{\text{avg}}}^{m+N_{\text{avg}}} \xi_j(i) \quad (9)$$

where $2N_{\text{avg}} + 1$ is the average size of the sliding window.

Using the estimated channel, EGC can be employed with time-domain despreading to accumulate useful signals from different OFCDM symbols. The EGC weight is given by

$$\hat{\varphi}_m(i) = \frac{\hat{H}_m^*(i)}{\left| \hat{H}_m(i) \right|} \quad (10)$$

where $(\cdot)^*$ stands for the conjugate operation. After EGC of the zeroth to $(N_T - 1)$th OFCDM symbol, the resultant signal of the $\overline{k}$th code channel on the mth subcarrier is given by

$$\begin{aligned} \gamma_{\overline{k},m} &= \frac{1}{N_T} \sum_{i=0}^{N_T-1} r_{m,i} \hat{\varphi}_m(i) c_{N_T,i}^{(\overline{k}_T)} s_{m,i} \\ &= \sqrt{P_d} d_{\overline{k},m} c_{N_F,m}^{(\overline{k}_F)} \alpha_m + MCI_{\overline{k},m}^{(F)} + \eta_{\overline{k},m} \end{aligned} \quad (11)$$

where $\alpha_m = (1/N_T) \sum_{i=0}^{N_T-1} H_m(i) \hat{\varphi}_m(i)$ is the channel factor on the mth subcarrier after EGC, and $d_{\overline{k},m} = d_{\overline{k},m,i}$ for $i = 0, 1, \cdots, N_T - 1$. The first term on the right-hand side of (11) is the useful signal, $MCI_{\overline{k},m}^{(F)}$ is the MCI in frequency-domain, generated by code channels in Ω_F, and $\eta_{\overline{k},m}$ is the additive noise.

B. Pure MMSE Detection

As explained before, in a broadband channel, MCI in frequency-domain is serious. Pure MMSE detection is employed in frequency-domain at the zeroth stage. To recover the data symbol of the $\overline{k}$th code channel $d_{\overline{k}}$, where $d_{\overline{k}} = d_{\overline{k},m}$ for the concerned N_F subcarriers, a set of weighting factors are needed which should satisfy the MMSE criterion

$$\min_{w_m(\overline{k})} E \left\{ \left| \sqrt{P_d} d_{\overline{k}} - \sum_{m=0}^{N_F-1} w_m(\overline{k}) \gamma_{\overline{k},m} \right|^2 \right\}. \quad (12)$$

It is difficult to obtain a closed-form solution of (12). However, in case of full load, i.e., all N_F frequency-domain spreading codes are assigned for data transmission (each code channel has the same power), a simplified MMSE is obtainable due to the orthogonal property of OVSF codes. In practical applications, the exact MMSE weights should be different from

the simplified weights obtained under the assumption of full load. Nevertheless, since a high load is expected in high-speed data communications, the simplified version of the pure MMSE weighting factor is approximated as

$$w_m(\overline{k}) = \frac{E\left\{\sqrt{P_d}d_{\overline{k}}\gamma^*_{\overline{k},m}\middle|\alpha_m\right\}}{E\left\{|\gamma_{\overline{k},m}|^2\middle|\alpha_m\right\}} = \frac{P_d\alpha^*_m c^{(\overline{k}_F)}_{N_F,m}}{(K_C+1)P_d|\alpha_m|^2+\sigma^2} \tag{13}$$

where K_C is the number of code channels in Ω_F and σ^2 is the variance of the additive noise.

C. Hybrid MCI Cancellation and MMSE Detection

When multistage MCI cancellation is employed, the MMSE weight in (13) should be updated due to the reduction of MCI stage by stage. Using the signal replicas of interfering data channels ($I^{(s-1)}_{k,m}$, $k \in \Omega_F$) at the previous stage, the MCI in frequency-domain for the $\overline{k}$th data channel can be regenerated, which is given by

$$\mathrm{MCI}^{(s)}_{\overline{k},m} = \sum_{k\in\Omega_F} I^{(s-1)}_{k,m} = \sum_{k\in\Omega_F} \sqrt{P_d}\hat{d}^{(s-1)}_k c^{(k_F)}_{N_F,m}\hat{\alpha}_m \tag{14}$$

where $\hat{d}^{(s-1)}_k$ denotes the tentative hard data decision at the $(s-1)$th stage for the kth data channel, and $\hat{\alpha}_m = (1/N_T)\sum_{i=0}^{N_T-1}|\hat{H}_m(i)|$ is the estimated channel factor of the mth subcarrier. As shown in Fig. 2, at the sth stage, the regenerated MCI for the $\overline{k}$th data channel $\mathrm{MCI}^{(s)}_{\overline{k},m}$ is removed from the input signal $\gamma_{\overline{k},m}$, and the resultant signal is given by

$$\begin{aligned}\gamma^{(s)}_{\overline{k},m} &= \gamma_{\overline{k},m} - \mathrm{MCI}^{(s)}_{\overline{k},m} \\ &= \underbrace{\sqrt{P_d}d_{\overline{k}}c^{(\overline{k}_F)}_{N_F,m}\alpha_m}_{\text{useful signal}} \\ &\quad + \underbrace{\sum_{k\in\Omega_F}\left[\sqrt{P_d}d_k\alpha_m - \sqrt{P_d}\hat{d}^{(s-1)}_k\hat{\alpha}_m\right]c^{(k_F)}_{N_F,m}}_{\text{residual MCI}} \\ &\quad + \eta_{\overline{k},m}.\end{aligned} \tag{15}$$

It can be seen from (15) that the residual MCI on the sth stage depends on the reliability of $\hat{d}^{(s-1)}_k$ and the quality of the channel estimation $\hat{H}_m(i)$ because of $\hat{\alpha}_m$.

After MCI cancellation, the MMSE weights of the hybrid detection should be updated and given by

$$w^{(s)}_m(\overline{k}) = \frac{E\left\{\sqrt{P_d}d_{\overline{k}}\left(\gamma^{(s)}_{\overline{k},m}\right)^*\middle|\alpha_m\right\}}{E\left\{\left|\gamma^{(s)}_{\overline{k},m}\right|^2\middle|\alpha_m\right\}} = \frac{P_d\alpha^*_m c^{(\overline{k}_F)}_{N_F,m}}{E\left\{\left|\gamma^{(s)}_{\overline{k},m}\right|^2\middle|\alpha_m\right\}}. \tag{16}$$

Setting $\gamma^{(0)}_{\overline{k},m} = \gamma_{\overline{k},m}$ for $\overline{k} = 0,\cdots,K-1$, the pure MMSE weights in (13) can be obtained from (16) as $w^{(0)}_m(\overline{k})$. In practice, $w^{(s)}_m(\overline{k})$ $(s \geq 0)$ can be obtained by estimating $E\{|\gamma^{(s)}_{\overline{k},m}|^2|\alpha_m\}$. First of all, since there are totally N_d OFCDM symbols in time-domain, the output of the time-domain despreader of the (jN_T)th to the $[(j+1)N_T-1]$th OFCDM symbols is denoted as $\gamma^{(s)}_{\overline{k},m}(j)$, where $j = 0,\cdots,(N_d/N_T)-1$. Actually, $\gamma^{(s)}_{\overline{k},m}$ in (15) corresponds to $\gamma^{(s)}_{\overline{k},m}(0)$. Then, it is assumed that the residual MCIs on all data channels have the same variance. Moreover, due to the high correlation between channel fading among adjacent OFCDM symbols and subcarriers, over the time window from the $(j-I_{\mathrm{Tavg}})$th to the $(j+I_{\mathrm{Tavg}})$th signals after EGC, the channel fading factors on the $(m-I_{\mathrm{Favg}})$th to the $(m+I_{\mathrm{Favg}})$th subcarriers are assumed to be the same. Therefore, $E\{|\gamma^{(s)}_{\overline{k},m}|^2|\alpha_m\}$ can be approximated as

$$\begin{aligned}E\left\{\left|\gamma^{(s)}_{\overline{k},m}\right|^2\middle|\alpha_m\right\} &\approx \frac{1}{K(2I_{\mathrm{Tavg}}+1)(2I_{\mathrm{Favg}}+1)} \\ &\quad\times\sum_{\overline{k}=0}^{K-1}\sum_{j'=j-I_{\mathrm{Tavg}}}^{j+I_{\mathrm{Tavg}}}\sum_{m'=m-I_{\mathrm{Favg}}}^{m+I_{\mathrm{Favg}}}\left|\gamma^{(s)}_{\overline{k},m'}(j')\right|^2\end{aligned} \tag{17}$$

where $2I_{\mathrm{Tavg}}+1$ and $2I_{\mathrm{Favg}}+1$ are the average window sizes over time and frequency-domains, respectively. Since P_d and $c^{(\overline{k}_F)}_{N_F,m}$ are known, and $H_m(i)$ is estimated as $\hat{H}_m(i)$, $w^{(s)}_m(\overline{k})$ can be approximated as

$$\begin{aligned}w^{(s)}_m(\overline{k}) &\approx \frac{P_d\left(\sum_{i=0}^{N_T-1}\left|\hat{H}_m(i)\right|\right)K(2I_{\mathrm{Tavg}}+1)(2I_{\mathrm{Favg}}+1)}{N_T\sum_{\overline{k}=0}^{K-1}\sum_{j'=j-I_{\mathrm{Tavg}}}^{j+I_{\mathrm{Tavg}}}\sum_{m'=m-I_{\mathrm{Favg}}}^{m+I_{\mathrm{Favg}}}\left|\gamma^{(s)}_{\overline{k},m'}(j')\right|^2} \\ &\quad\times c^{(\overline{k}_F)}_{N_F,m}.\end{aligned} \tag{18}$$

By means of the estimated MMSE weights $w^{(s)}_m(\overline{k})$ the hybrid detection can be carried out. The resultant signals are further processed by the soft demodulator and turbo decoder. Finally, based on the decoding output, the new MCI to be used for next stage will be regenerated.

IV. Simulation Results

A. Configurations

Computer simulation is carried out to show the performance of hybrid MCI cancellation and MMSE detection in the turbo-coded OFCDM system. The major radio link parameters are given in Table I. The effective bandwidth is 101.5 MHz. Based on the optimization to compensate for the maximum multipath delay and to avoid the influence of Doppler shift, the number of subcarriers M_C is chosen to be 768 with the subcarrier spacing of 131.836 kHz. The number of IFFT points M is set to 1024. Therefore, the sampling rate after IFFT is $101.5 \times 1024/768 = 135$ Ms/s. A guard interval of 226 samples, or $T_g = 1.67$ μs, equivalently, is assigned between two OFCDM symbols. The packet length is 0.444 ms, which is composed of $N_d = 48$ OFCDM symbols per subcarrier. Setting the time-domain spreading factor of pilot channel $N_{T,P}$ to 16, there are $48/16 = 3$ pilot symbols on each subcarrier in one packet duration. For data channel, the spreading factor in time-domain N_T can be 4, 8, or 16. Information bits transmitted on each data channel are individually encoded by a turbo code of 1/2 rate. On the receiver side, the Max_Log_MAP algorithm is employed in the soft demodulator and turbo decoder (with iterative structure). Furthermore, a general exponential decay

TABLE I
SIMULATION PARAMETERS

Bandwidth/Baseband sampling rate		101.5MHz/135Msps
Number of sub-carriers (M_c)		768
Number of IFFT/FFT points		1024
Complete OFCDM symbol duration (Effective data + Guard interval)		9.259 μs (7.585+1.674 μs)
Packet length (No. of OFCDM symbols per sub-carrier)		0.444ms (N_d=48 OFCDM symbols)
Spreading code	Channelization code	2-D OVSF
	Scrambling code	Pseudo random code
Modulation	Data	QPSK, 16QAM
	Pilot	QPSK
Spreading length	Data	N_T=4, 8, or 16 , $N_F \geq 1$
	Pilot	$N_{T,P}$=16 (code-multiplexed)
Channel estimation		Pilot-aided
Despreading		EGC in time domain and hybrid detection in frequency domain
Demodulation		Soft demodulation (Max_Log_MAP)
Channel coding / decoding		1/2 rate turbo / Iterative Max_Log_MAP decoding
Channel parameters		Paths: 12, Path separation: $0.1481\mu s$ ($20T_s$)

multipath model is considered with 12 paths and an equal separation of $20T_s$ between adjacent paths. The power difference between adjacent paths is set to 1 dB, and the total power in the power delay profile is one. Doppler shift f_D is 50 Hz. In computer simulations, a modified Jake's model [9] is employed to generate multiple uncorrelated paths. Finally, the effective signal-to-noise ratio (SNR) per information bit is defined as $SNR_b = P_d N(1+\beta/K)/Q_b R_{eff}\sigma_n^2$, where Q_b is 2 for QPSK and 4 for 16 QAM, R_{eff} is the effective code rate and σ_n^2 is the variance of the channel noise.

B. Effect of System Parameters

Unless noted otherwise, the following parameters are used. The 2-D spreading factor is $N = 8\times 8$ and the number of data channels is $K = 56$. The power ratio β/K between the pilot and all data channels is set to 0.20. The iterations in turbo decoding are two. The average window size in frequency-domain for channel estimation is $2N_{\text{avg}}+1 = 3$. The average window sizes in time and frequency-domain for MMSE weight estimates are $2I_{\text{Tavg}}+1 = 3$ and $2I_{\text{Favg}}+1 = 3$, respectively. Finally, the parity bits of turbo codes are obtained directly from decoding for the MCI regeneration. First of all, the packet error rate (PER) performance of the turbo-coded OFCDM system is shown in Fig. 3 as a function of SNR_b, when both hybrid detection and pure MMSE are employed. It can be seen that for both modulation schemes, the PER decreases as the number of stages increases due to the reduction of MCI in each stage, especially when SNR_b is large. The most significant reduction in PER is obtained from the zeroth stage to the first stage, then the reduction becomes smaller as the number of stages increases. The hybrid detection works much more effectively in 16 QAM than in QPSK. This is because 16 QAM is more vulnerable to MCI than QPSK, so significant improvement can be obtained in 16 QAM by using hybrid detection. Although the PER performance gets better when the number of stages increases, the improvement becomes insignificant after the second stage for QPSK and fifth stage

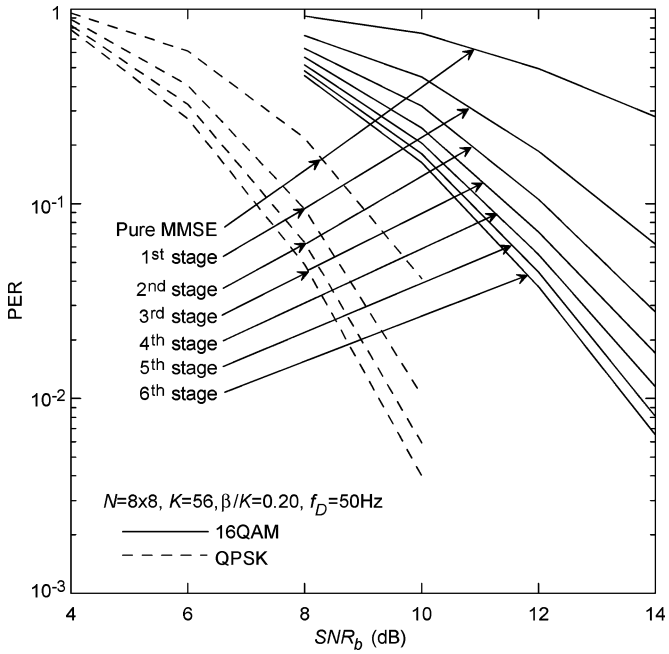

Fig. 3. System performance of pure MMSE and hybrid detection.

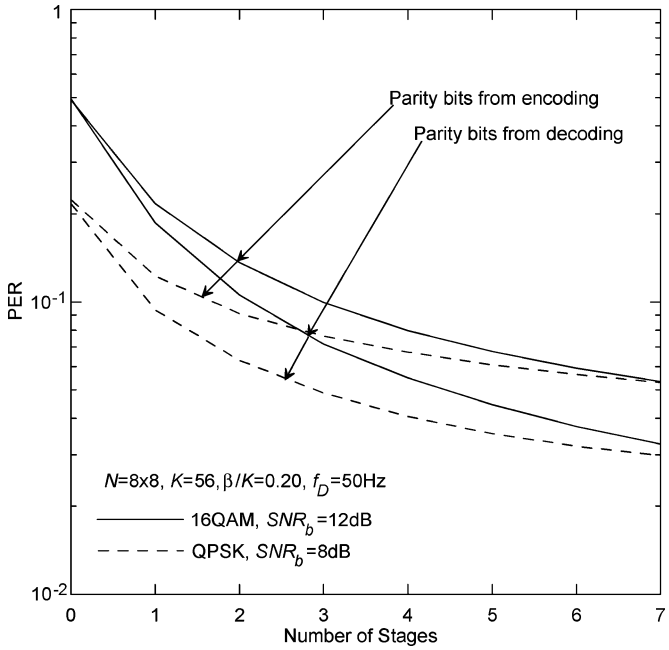

Fig. 4. System performance for different parity-bit recovery schemes.

for 16 QAM. Therefore, the hybrid detection with two stages is sufficient for QPSK, while the hybrid detection with five stages is necessary for 16 QAM.

As described in Section II, the parity bits can be obtained by either encoding recovered systematic bits or by modifying turbo decoding algorithm. Given $\text{SNR}_b = 8$ B and 12 dB for QPSK and 16 QAM, respectively, Fig. 4 compares the system performance for different parity-bit recovery schemes from encoding and directly from decoding, as a function of the number of stages. It can be seen that for either QPSK or 16 QAM, the performance of using parity bits directly from decoding is better than indirectly from encoding. This is because when the parity bits are obtained from encoding, the errors in the systematic bits

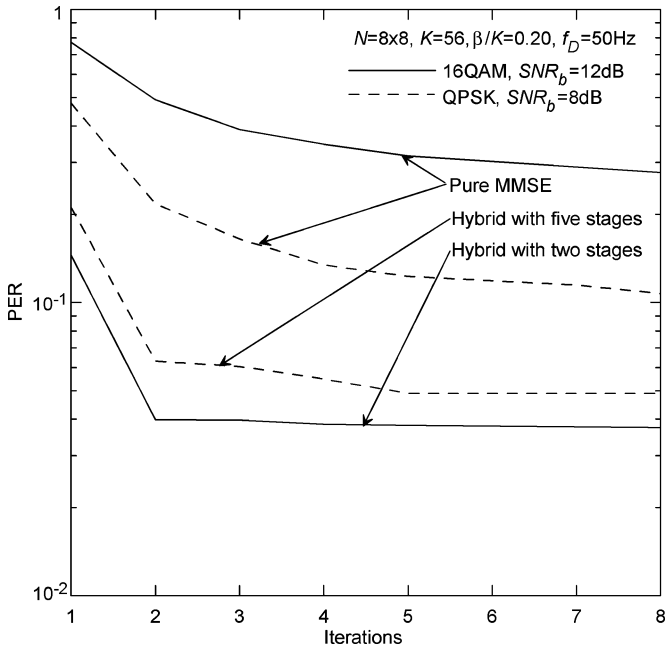

Fig. 5. System performance as a function of iterations in turbo decoding.

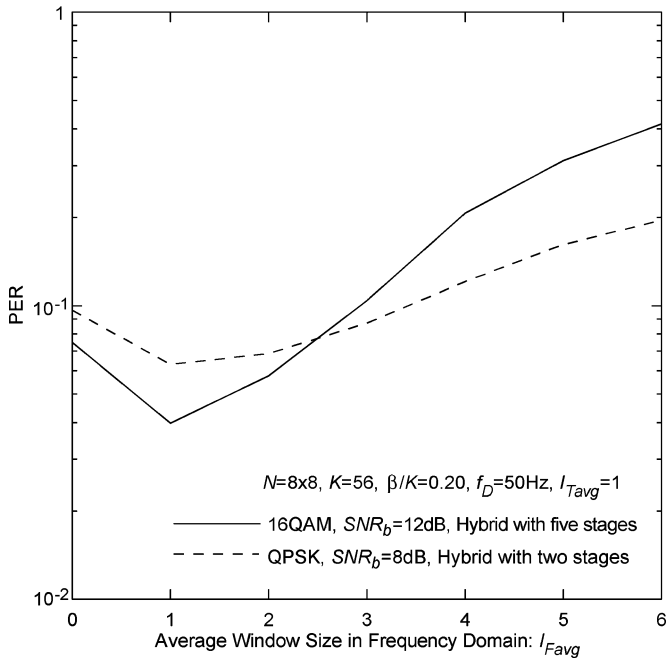

Fig. 6. Effect of I_{Favg} on the system performance.

will propagate into parity bits due to the recursive systematic encoding. The effect of error propagation accumulates as the iterative MCI cancellation goes on, and the performance gap between both schemes increases with stages increasing. Therefore, to get better performance, parity bits should be recovered directly from decoding algorithms which avoids the error propagation.

Using the hybrid detection of two stages and five stages for QPSK and 16QAM, respectively, the PER performance is shown in Fig. 5 as a function of the number of iterations in turbo decoding. The system performance of the pure MMSE is also shown as a comparison. It can be seen that the PER performance of the pure MMSE improves gradually as the number of iterations increases. However, in the hybrid detection, a sharp reduction in PER is observed from the first iteration to the second iteration, afterwards the PER curve tends to be flat. Using the pure MMSE, at least four iterations are needed, while using the hybrid detection, two iterations are sufficient to provide good performance for the turbo-coded OFCDM system. This is because for the pure MMSE (or the hybrid detection with the zeroth stage) there is too much MCI so that turbo decoding needs more iterations. However, for the hybrid detection with more stages, much MCI has been cancelled out, and few iterations (i.e., two iterations) are sufficient.

In real applications, the MMSE weights are estimated by using (18). Given $f_D = 50$ Hz and $I_{\mathrm{Tavg}} = 1$, Fig. 6 illustrates the system performance as a function of I_{Favg}. When I_{Favg} increases first from zero to one, the PER decreases because the noise in weight estimation is reduced. However, when I_{Favg} is increased beyond one, the system performance degrades. This is because the broadband channel is highly frequency selective. When I_{Favg} is large, the correlation among the $(2I_{\mathrm{Favg}} + 1)$ subcarriers decreases, and the distortion of the weight estimation is introduced. In the slow fading and $I_{\mathrm{Tavg}} = 1$, the optimal I_{Favg} achieving the lowest PER is one for both 16 QAM and QPSK.

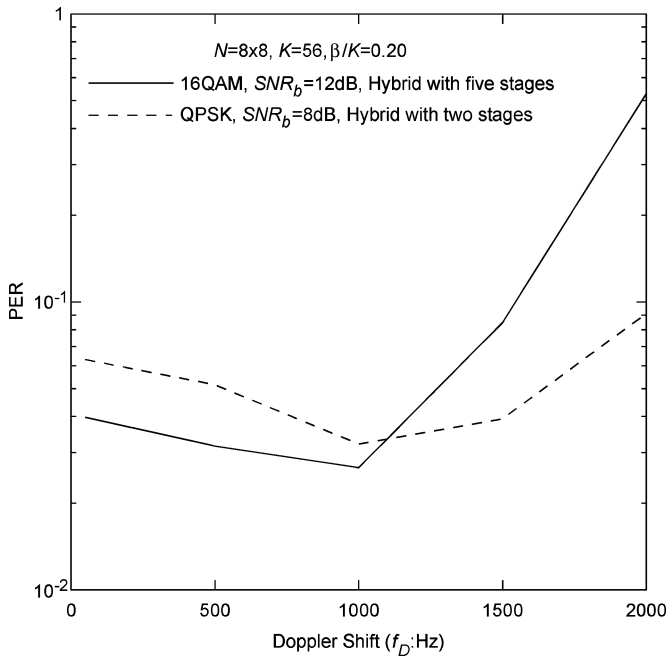

Fig. 7. System performance of the hybrid detection as a function of Doppler shift.

When fast fading occurs, the channel variation in one packet duration is serious. For example, for a carrier frequency of 5 GHz, when a mobile terminal moves at a speed of 300 km/h, the resultant maximum Doppler shift can be as high as 1500 Hz. Therefore, it is necessary to investigate the effect of Doppler shift (f_D) on the system performance. Fig. 7 shows the PER performance of the hybrid detection as a function of the Doppler shift. Note that the concerned system employs EGC in time-domain, and the hybrid detection is only carried out in frequency-domain. It can be seen that the PER decreases with f_D increasing from 50 Hz and reaches a minimal value when f_D is around 1000 Hz for both QPSK and 16 QAM. This is because although the MCI in time-domain increases with f_D,

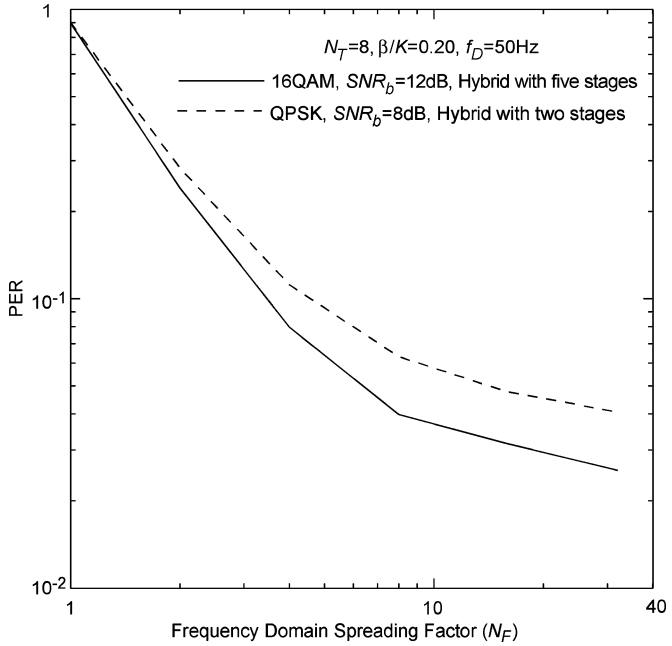

Fig. 8. System performance as a function of the frequency-domain spreading factor.

the channel estimation algorithm with linear interpolation can still track the channel variation. With good channel estimation, MCI cancellation works effectively in frequency-domain and the time-domain diversity gain is obtained. When the gain from time diversity overcomes the loss due to increased MCI in time-domain, the system performance is enhanced. However, if f_D increases further, the system performance degrades rapidly. This is because when f_D is too large, the channel varies so fast that the channel estimation algorithm cannot track the changes. Without precise channel estimation, the hybrid detection fails to work well and the PER is increased dramatically. In summary, the turbo-coded OFCDM system with hybrid detection is robust to channel variations when f_D is less than 1500 Hz.

Finally, for a fixed time-domain spreading factor $N_T = 8$ and system load $K/N = (N_T - 1)/N_T = 0.875$, Fig. 8 shows the PER performance as a function of the frequency-domain spreading factor N_F. It can be seen that the system performance is poor when $N_F = 1$. This is because there is no frequency diversity gain although there is no MCI in frequency-domain. As N_F increases, the PER decreases rapidly at first, then the PER drops slowly when N_F is large. This is because when N_F increases from a small value, the frequency diversity gain is large and overcomes the increased MCI in frequency-domain. However, as N_F increases further, the frequency spacing of two closest subcarriers in the N_F subcarriers reduces due to the fixed bandwidth, and the correlation among the N_F subcarriers becomes high. Therefore, the frequency diversity gain is saturated. Although there is still reduction in PER when N_F is large, the performance is almost saturated when N_F is 16 for both QPSK and 16 QAM schemes.

V. Conclusion

The performance of the downlink turbo-coded OFCDM system is investigated in this paper with hybrid MCI cancellation and MMSE detection. The following conclusions are drawn.

1) The hybrid detection outperforms pure MMSE. The performance improves as the number of stages increases. For QPSK, the hybrid detection of two stages is sufficient, while for 16 QAM, the hybrid detection of five stages is necessary. The hybrid detection works more effectively for 16 QAM than for QPSK.
2) To carry out interference regeneration for the hybrid detection, the conventional decoding algorithm of turbo codes which only decodes systematic bits should be extended to decode parity bits as well. Furthermore, in the pure MMSE, at least four iterations are needed in the turbo decoding to provide stable performance, while only two iterations are sufficient in the hybrid detection.
3) The proposed method for MMSE weight estimation (see (18)) works well with proper values of the average window size in time-domain (I_{Tavg}) and in frequency-domain (I_{Favg}). To achieve good performance, $I_{\mathrm{Tavg}} = 1$ and $I_{\mathrm{Favg}} = 1$ should be selected over slow fading channels.
4) Given N_T, the system performance improves as N_F increases. However, the performance gain is saturated when N_F is large than 16.

References

[1] H. Atarashi, S. Abeta, and M. Sawahashi, "Variable spreading factor-orthogonal frequency and code division multiplexing (VSF-OFCDM) for broadband packet wireless access," *IEICE Trans. Commun.*, vol. E86-B, pp. 291–299, Jan. 2003.
[2] F. Adachi, M. Sawahashi, and H. Suda, "Wideband DS-CDMA for next-generation mobile communications systems," *IEEE Commun. Mag.*, vol. 36, no. 9, pp. 56–69, Sep. 1998.
[3] Y. Kishiyama, N. Maeda, H. Atarashi, and M. Sawahashi, "Investigation of optimum pilot channel structure for VSF-OFCDM broadband wireless access in forward link," in *Proc. IEEE Veh. Technol. Conf.-Spring*, Apr. 2003, pp. 139–144.
[4] Y. Q. Zhou, J. Wang, and M. Sawahashi, "Downlink transmission of broadband OFCDM systems—Part I: Hybrid detection," *IEEE Trans. Commun.*, vol. 53, pp. 718–729, Apr. 2005.
[5] C. Berrou and A. Glavieux, "Near optimum error correcting coding and decoding: Turbo-codes (1)," in *Proc. IEEE Int. Commun. Conf.*, May 1993, pp. 1064–1070.
[6] N. Maeda, H. Atarashi, and M. Sawahashi, "Performance comparison of channel interleaving methods in frequency-domain for VSF-OFCDM broadband wireless access in forward link," *IEICE Trans. Commun.*, vol. E86-B, pp. 300–313, Jan. 2003.
[7] S. A. Barbulescu, W. Farrell, P. Gray, and M. Rice, "Bandwidth efficient turbo coding for high speed mobile satellite communications," in *Proc. Int. Symp. Turbo Codes*, Brest, France, Sep. 1997, pp. 119–126.
[8] P. Roberson, "Illuminating the structure of code and decoder of parallel concatenated recursive systematic (turbo) codes," in *Proc. IEEE GLOBECOM*, Dec. 1994, pp. 1298–1303.
[9] P. Dent, G. E. Bottomley, and T. Croft, "Jakes fading model revisited," *Electron. Lett.*, vol. 29, pp. 1162–1163, Jun. 1993.

Yiqing Zhou (M'04) was born in Zhejiang, China, in 1975. She received the B.S. degree in communication and information engineering, the M.S. degree in signal and information processing from the Southeast University, Nanjing, China, in 1997 and 2000, respectively, and the Ph.D. degree in electrical and electronic engineering from the University of Hong Kong, Hong Kong, in 2004.

Since 2004, she has been with the Department of Electrical and Electronic Engineering, University of Hong Kong, as a Postdoctoral Fellow. Her research interests include coding theory, spread-spectrum, OFDM systems, interference cancellation, hybrid ARQ, and other transmission techniques for wireless high-speed data communications.

Jiangzhou Wang (M'91–SM'94) received the B.S. and M.S. degrees from Xidian University, Xian, China, in 1983 and 1985, respectively, and the Ph.D. degree (with Greatest Distinction) from the University of Ghent, Ghent, Belgium, in 1990, all in electrical engineering.

From 1990 to 1992, he was a Postdoctoral Fellow at the University of California, San Diego, where he worked on the research and development of cellular CDMA systems. From 1992 to 1995, he was a Senior System Engineer at Rockwell International Corporation, Newport Beach, CA, where he worked on the development and system design of wireless communications. Since 1995, he has been with the University of Hong Kong, where he is currently an Associate Professor and the Coordinator of the Telecommunications Group. He has held a Visiting Professor position at NTT DoCoMo, Inc., Kanagawa, Japan. He has written/edited *Broadband Wireless Communications* (Kluwer, 2001) and *Advances in 3G Enhanced Technologies for Wireless Communications* (Artech House, 2002), respectively. He holds one U.S. patent in the GSM system.

Dr. Wang was a Technical Chairman of the IEEE Workshop on 3G Mobile Communications, 2000. He has published over 100 papers, including more than 30 IEEE TRANSACTIONS/JOURNAL papers in the areas of wireless mobile and spread-spectrum communications. He is an Editor for the IEEE TRANSACTIONS ON COMMUNICATIONS and a Guest Editor for the IEEE JOURNAL ON SELECTED AREAS IN COMMUNICATIONS (Wideband CDMA, 2000 and 2001, and Advances in Multicarrier CDMA, 2006). He is listed in *Who's Who in the World*.

Mamoru Sawahashi (M'88) received the B.S. and M.S. degrees from Tokyo University, Tokyo, Japan, in 1983 and 1985, respectively, and the Dr. Eng. degree from the Nara Institute of Technology, Nara, Japan, in 1998.

In 1985, he joined NTT Electrical Communications Laboratories, and in 1992, he transferred to NTT Mobile Communications Network, Inc. (now, NTT DoCoMo, Inc.), Kanagawa, Japan. Since joining NTT, he has been engaged in the research of modulation/demodulation techniques for mobile radio, and research and development of wireless access technologies for W-CDMA mobile radio and broadband wireless packet access technologies for beyond IMT-2000. He is now the Director of the IP Radio Network Development Department, NTT DoCoMo, Inc.

Dr. Sawahashi is currently serving as an Editor for the IEEE TRANSACTIONS ON WIRELESS COMMUNICATIONS and a Guest Editor for the IEEE JOURNAL ON SELECTED AREAS IN COMMUNICATIONS.